Time evolution of interacting vortices under overdamped motion

Mauricio S. Ribeiro,[1,*] Fernando D. Nobre,[1,†] and Evaldo M. F. Curado[1,2,‡]

[1]*Centro Brasileiro de Pesquisas Físicas and National Institute of Science and Technology for Complex Systems, Rua Xavier Sigaud 150, Rio de Janeiro, RJ 22290-180, Brazil*

[2]*Laboratoire APC, Université Paris Diderot, 10 rue A. Domon et L. Duquet, 75205 Paris, France*

(Received 15 December 2011; published 27 February 2012)

A system of interacting vortices under overdamped motion, which has been commonly used in the literature to model flux-front penetration in disordered type-II superconductors, was recently related to a nonlinear Fokker-Planck equation, characteristic of nonextensive statistical mechanics, through an analysis of its stationary state. Herein, this connection is extended by means of a thorough analysis of the time evolution of this system. Numerical data from molecular-dynamics simulations are presented for both position and velocity probability distributions $P(x,t)$ and $P(v_x,t)$, respectively; both distributions are well fitted by similar q-Gaussian distributions, with the same index $q = 0$, for all times considered. Particularly, the evolution of the system occurs in such a way that $P(x,t)$ presents a time behavior for its width, normalization, and second moment, in full agreement with the analytic solution of the nonlinear Fokker-Planck equation. The present results provide further evidence that this system is deeply associated with nonextensive statistical mechanics.

DOI: 10.1103/PhysRevE.85.021146 PACS number(s): 05.40.Fb, 05.10.Gg, 05.20.−y

I. INTRODUCTION

The use of nonlinear (NL) equations in physics has opened the possibility of an appropriate description of a wide range of real phenomena in recent years [1,2]. Many physical systems exhibit complicated collective behavior associated with NL phenomena, e.g., those characterized by spatial disorder, due to some type of inhomogeneous media, or those with long-range interactions and/or strong correlations among particles. Considerable advances have been attained recently in the study of NL equations, essentially due to the latest advances in computer technology, since in many cases these equations have to be investigated numerically.

Two of the most studied NL differential equations are generalizations of the Schrödinger [3] and Fokker-Planck equations [4]. In both cases, the NL contributions lead to important novel insights, which are relevant for modeling several new physical aspects. In the most common formulation of the NL Schrödinger equation, one introduces a new cubic term in the wave function, which, for some particular type of solution, is responsible for the modulation of the wave function. Such a procedure, characterized by the addition of extra NL terms, has been much used in the literature for constructing such equations. A different approach consists of transforming one or more linear terms into NL ones, as usually happens in generalized Fokker-Planck equations [4]. This later procedure has been used in a recent generalization of important equations of quantum physics, and particularly in a new proposal of a NL Schrödinger equation, which also presents a modulation for the wave function [5].

Among nonlinear Fokker-Planck equations (NLFPEs), we focus on the one usually associated with nonextensive statistical mechanics [6]. Defining the probability $P(x,t)$ for finding a given particle at a position x in time t, this equation is given by [7,8]

$$\eta \frac{\partial P(x,t)}{\partial t} = -\frac{\partial [A(x)P(x,t)]}{\partial x} + D\nu \frac{\partial}{\partial x}\left\{ [L_0 P(x,t)]^{\nu-1} \frac{\partial P(x,t)}{\partial x} \right\}, \quad (1)$$

where η and D represent the friction and diffusion constants, respectively, and $A(x) = -d\phi(x)/dx$ is an external force associated with a confining potential. From the normalization condition $\int_{-\infty}^{\infty} dx\, P(x,t) = 1$, one readily sees that $P(x,t)$ presents dimension (length)$^{-1}$; therefore, the argument of the nonlinear term, introduced herein by means of the real exponent ν, should be dimensionless. The length scale L_0, which should appear naturally from the physical system considered,[1] is introduced in order to yield the correct dimensions for Eq. (1); this difficulty does not occur in the particular case $\nu = 1$, i.e., in the corresponding linear equation [9]. This NLFPE was solved for an external harmonic force, $A(x) = -\alpha x$ ($\alpha \geqslant 0$), the initial condition $P(x,0) = \delta(x)$, and $\eta = L_0 = 1$ (i.e., for a conveniently rescaled dimensionless probability) [7,8]:

$$P(x,t) = B(t)[1 - \beta(t)(\nu - 1)x^2]_+^{\frac{1}{\nu-1}}, \quad (2)$$

where $[y]_+ = y$, for $y > 0$, and zero otherwise. From the equation above one readily identifies the q-Gaussian distribution of nonextensive statistical mechanics if $\nu = 2 - q$ [6]. To guarantee the normalization of the probability for any time t,

*ribeiro@cbpf.br
†fdnobre@cbpf.br
‡evaldo@cbpf.br

[1]Although one could think of more general physical situations, defined in terms of various independent length scales, our main interest herein concerns an application characterized by a single length scale.

the time-dependent parameters $B(t)$ and $\beta(t)$ should be directly related to their values at some reference time t_0,

$$\frac{\beta(t)}{\beta(t_0)} = \left[\frac{B(t)}{B(t_0)}\right]^2, \tag{3}$$

with the normalization factor $B(t)$ being given by

$$B(t) = B(t_0)\left[\frac{1}{K_2} + \left(1 - \frac{1}{K_2}\right)e^{-\frac{t}{\tau}}\right]^{-\frac{1}{1+\nu}}, \qquad \tau = \frac{1}{\alpha(1+\nu)}, \tag{4}$$

and

$$K_2 = \frac{\alpha}{2\nu D\beta(t_0)[B(t_0)]^{\nu-1}}. \tag{5}$$

From the probability distribution of Eq. (2) one can find its moments; particular attention is usually given to the second moment [10],

$$\langle x^2\rangle \propto \{1 - \exp[-\alpha(1+\nu)t]\}^{\frac{2}{1+\nu}}, \tag{6}$$

which is finite for $\nu > 1/3$. For times much smaller than those characteristic of the approach to the stationary state ($t \ll 1$), one gets an evolution ruled by anomalous diffusion, $\langle x^2\rangle \propto t^{\frac{2}{\nu+1}}$, representing a signature of the NLFPE in Eq. (1). At longer times, one gets a crossover to a different evolution, characteristic of the approach to the stationary state [10].

One important consequence from NLFPEs is the H theorem [4,10–17]. For a system in contact with a thermal bath this theorem concerns a well-defined sign for the time derivative of the free energy, $(dF/dt) \leqslant 0$:

$$F = U - \gamma S, \qquad U = \int_{-\infty}^{\infty} dx\, \phi(x) P(x,t), \tag{7}$$

with γ representing a positive Lagrange multiplier. The entropy may be defined in a very general form,

$$S[P] = \frac{1}{L_0}\int_{-\infty}^{\infty} dx\, g[L_0 P(x,t)], \qquad g(0) = g(1) = 0, \qquad \frac{d^2 g}{d(L_0 P)^2} \leqslant 0, \tag{8}$$

where the functional $g[L_0 P(x,t)]$ presents units of entropy. In order to satisfy $(dF/dt) \leqslant 0$, the NLFPE and the entropy must be related [4,10–17]; for the NLFPE in Eq. (1) one should have

$$g[L_0 P] = k\,\frac{[L_0 P(x,t)]^\nu - L_0 P(x,t)}{1-\nu}, \qquad S[P] = k\,\frac{1 - L_0^{\nu-1}\int_{-\infty}^{\infty} dx\,[P(x,t)]^\nu}{\nu - 1}, \tag{9}$$

where we defined $k = D/\gamma$. The extremization of the entropy above under the constraints of probability normalization, and the internal energy defined as in Eq. (7), lead to the probability distribution of Eq. (2).

Next, we will present a physical application characterized by a NLFPE and its associated entropy in the forms presented above, with an exponent $\nu = 2$ [18] (see also Ref. [19]). Since the distribution of Eq. (2) is identified as the q-Gaussian distribution of nonextensive statistical mechanics for $\nu = 2 - q$ [6], the corresponding distribution presents an index $q = 0$.[2] In this case, the entropy and the distribution are given, respectively, by

$$S[P] = k\left\{1 - L_0\int_{-\infty}^{\infty} dx\,[P(x,t)]^2\right\}, \tag{10}$$

$$P(x,t) = B(t)[1 - \beta(t)x^2]_+. \tag{11}$$

Moreover, the parameters $B(t)$ and $\beta(t)$ are related through [cf. Eqs. (3)–(5)],

$$B(t)\beta(t) = \frac{B(t_0)\beta(t_0)}{K_2}[1 + (K_2 - 1)e^{-3\alpha t}]^{-1} = a_0[1 + a_1 e^{-3\alpha t}]^{-1}, \tag{12}$$

$$a_0 = \frac{\alpha}{4D}, \quad a_1 = \frac{\alpha}{4D\beta(t_0)B(t_0)} - 1. \tag{13}$$

II. PHYSICAL APPLICATION: INTERACTING VORTICES UNDER OVERDAMPED MOTION

The physical system of interest consists of interacting vortices performing an overdamped motion, which has been used in the literature to model flux lines in disordered type-II superconductors (see, e.g., Refs. [20–23]). In a previous work [18], a very good agreement was found between the particle-position stationary-state distributions obtained by means of molecular-dynamics simulations and the solution of a NLFPE for both $T = 0$ and $T > 0$; the temperature T, which is associated with a linear-diffusion term, comes, as usual, from a thermal noise of a Langevin equation. In this case, it was shown that: (i) for $T = 0$ the data was well fitted by a q-Gaussian distribution with $q = 0$; (ii) the distribution changes due to the temperature, being given in terms of a W-Lambert function for $T > 0$; and (iii) for sufficiently high values of T one recovers a Gaussian distribution. In the present study we will restrict ourselves to $T = 0$, i.e., no thermal noise. We will provide further evidence that the connection of case (i) holds also during the whole time evolution of the system. Moreover, similar q-Gaussian distributions are found for the particle velocities.

The equation of motion of a flux line i under overdamped motion [i.e., with $(d\mathbf{v}_i/dt) = 0$], in a medium with an effective friction coefficient η, may be written as

$$\eta\mathbf{v}_i = \mathbf{F}_i^{\rm pp} + \mathbf{F}_i^{\rm ext} \quad (i = 1,2,\ldots,N), \tag{14}$$

where $\mathbf{v}_i$ stands for its velocity and the terms on the right-hand side depict the forces acting on the vortex. The first contribution, $\mathbf{F}_i^{\rm pp}$, takes into account the interactions among particles [each vortex interacts with the remaining $(N-1)$ vortices], whereas $\mathbf{F}_i^{\rm ext}$ represents an external force acting on vortex i. Although this problem can be formulated easily in a three-dimensional space, herein it will be discussed in two

[2] It is important to notice that the "duality" $q \leftrightarrow (2-q)$ between the distribution index $q = 0$ and the entropic index $\nu = 2$ occurs whenever the entropy is extremized by considering the energy definition in Eq. (7); equal indexes appear when one uses a generalized definition for the internal energy [6].

dimensions to conform with the numerical simulations that will be presented later. We consider

$$\mathbf{F}_i^{\rm pp} = \frac{1}{2}\sum_{j\neq i} B_{ij}^{\rm pp}(r_{ij})\,\hat{\mathbf{r}}_{ij}, \tag{15}$$

and as usual the factor $1/2$ compensates for the double counting of interactions. The distance between particles i and j is $r_{ij} = |\mathbf{r}_i - \mathbf{r}_j|$, and $\hat{\mathbf{r}}_{ij} = (\mathbf{r}_i - \mathbf{r}_j)/r_{ij}$ is a vector defined along the axis of each pair of particles. In the interactions above, $B^{\rm pp}(r_{ij}) = f_0 K_1(r_{ij}/\lambda)$, with K_1 representing a modified Bessel function of the second kind of order 1 and f_0 a positive constant. These interactions are defined in terms of a single characteristic length scale λ, known as the London penetration length. The vortex-vortex interactions $B_{ij}^{\rm pp}(r_{ij})$ are repulsive and radially symmetric, whereas the external forces $\mathbf{F}_i^{\rm ext}$ should be associated with a confining type of potential, so that the system can reach an stationary state after a sufficiently long time.

For a description in terms of continuous variables, we perform a coarse graining by introducing a local density of vortices at time t, $\rho(\mathbf{r},t)$, making use of the continuity equation

$$\frac{\partial\rho(\mathbf{r},t)}{\partial t} = \nabla\cdot\mathbf{J}, \tag{16}$$

and defining the current density, $\mathbf{J} = \rho\mathbf{v}$. Supposing that the local density varies smoothly within the range of interactions $B_{ij}^{\rm pp}(r_{ij})$, one may consider $\rho(\mathbf{r},t) \approx \rho(0,t) + \mathbf{r}\cdot\nabla\rho(\mathbf{r},t)$, so that the effect of the remaining $(N-1)$ vortices on a given vortex may be written in terms of a mean force $\mathbf{F}^{\rm pp}$,

$$\begin{aligned}\mathbf{F}^{\rm pp} &= \frac{1}{2}\int d^2r\rho(\mathbf{r},t)B^{\rm pp}(r)\hat{\mathbf{r}}\\ &\approx \frac{1}{2}\int d^2r[\mathbf{r}\cdot\nabla\rho(\mathbf{r},t)]B^{\rm pp}(r)\hat{\mathbf{r}},\end{aligned} \tag{17}$$

where we have used the property that the integral over $\rho(0,t)$ yields zero, due to symmetry. Without loss of generality, we will take $\nabla\rho(\mathbf{r},t)$ along the x axis; in this way, one may see easily that the y component of $\mathbf{F}^{\rm pp}$ is zero, leading to a force acting along the same axis chosen for $\nabla\rho(\mathbf{r},t)$. Since the local density changes slowly within the range of interactions (which is typically of order λ), one may approximate the integral above by[3]

$$\mathbf{F}^{\rm pp} \approx a\nabla\rho(\mathbf{r},t); \quad a = \pi\int_0^\infty dr\, r^2 B^{\rm pp}(r), \tag{18}$$

and for the particle-particle interactions defined above, one has $a = 2\pi f_0\lambda^3$. Let us consider for the external forces on each particle $\mathbf{F}^{\rm ext} = -A(x)\hat{\mathbf{x}}$. Substituting these results into Eq. (16) and using Eq. (14), one gets

$$\begin{aligned}\eta\frac{\partial\rho(\mathbf{r},t)}{\partial t} &= \nabla\cdot\{\rho(\mathbf{r},t)[a\nabla\rho(\mathbf{r},t) + \mathbf{F}^{\rm ext}]\}\\ &= \frac{\partial}{\partial x}\left\{\rho(\mathbf{r},t)\left[a\,\frac{\partial\rho(\mathbf{r},t)}{\partial x} - A(x)\right]\right\},\end{aligned} \tag{19}$$

where $\rho(\mathbf{r},t) \equiv \rho(x,y,t)$ and we have used the fact that $\nabla\rho(\mathbf{r},t)$ is along the x-axis.[4] Since the spatial derivatives only operate on the x variable, one may consider the equation above for a fixed y [18,23]. Accordingly, defining the probability of finding a given particle with a coordinate x at time t as $P(x,t) = (L_y/N)\rho(x,t)$, one obtains

$$\begin{aligned}\eta\,\frac{\partial P(x,t)}{\partial t} &= -\frac{\partial[A(x)P(x,t)]}{\partial x}\\ &\quad + 2D\frac{\partial}{\partial x}\left\{[\lambda P(x,t)]\frac{\partial P(x,t)}{\partial x}\right\},\end{aligned} \tag{20}$$

where $D = (N\pi f_0\lambda^2)/L_y$. Comparing this NLFPE with the one of Eq. (1), one readily identifies the characteristic length $L_0 = \lambda$ and the exponent $\nu = 2$.

III. RESULTS

In order to compare time-dependent properties of the solution of the NLFPE in Eq. (19) [or equivalently, in Eq. (20)] with those of the above-mentioned physical system, we have performed molecular-dynamics simulations by integrating the N equations of motion defined in Eq. (14). Since this NLFPE was solved for an external harmonic force $A(x) = -\alpha x$ ($\alpha \geqslant 0$) and the initial condition $P(x,0) = \delta(x)$ [7,8], we will use the same confining potential and an initial condition for the particle positions as close as possible to this one in the following simulations. From now on, we will consider the friction coefficient $\eta = 1$ and all lengths will be given in units of λ. Except for the illustration in Fig. 1, all our simulations were carried for a system of $N = 4000$ particles. The particles were confined in a two-dimensional box of size $L_x = 280\lambda$ and $L_y = 20\lambda$, with periodic boundary conditions in the y direction; the restoring constant used was $\alpha = 10^{-3} f_0/\lambda$. According to Eqs. (11)–(13), the particular choice of α should only affect the time required for the approach to the stationary state, as well as the time evolution of parameters $B(t)$ and $\beta(t)$, but not the functional forms of $P(x,t)$ and $B(t)\beta(t)$. As an approximation to the initial condition $P(x,0) = \delta(x)$, the simulation starts at time $t = 0$ with the particles confined according to a "water-bag" distribution (all particles uniformly distributed in a narrow region around $x = 0$); this condition is commonly used in numerical solutions of Fokker-Planck equations [10]. In order to reduce a dependence on the particular initial distribution of particles, averages were carried over 100 samples. Due to this confinement of particles, the effect of the harmonic potential is very weak initially, and the repulsive interactions dominate, making the particles move away rapidly from the origin. Then the confining potential starts playing an important role, decreasing the velocities of the particles in such a way that after a sufficiently long time the forces on each particle cancel, with the system attaining a

[3]The present approximations are expected to yield small discrepancies with respect to the results obtained from the molecular-dynamics simulations, as will be verified later on.

[4]We call attention to the fact that the calculated parameter herein, $a = 2\pi f_0\lambda^3$, corresponds to twice the one of Ref. [18]. In fact there are a few misprints in Eqs. (12) and (13) of this reference, where the following changes should be made: (i) in the left-hand side of Eq. (12), $a \to 2a$; (ii) in the right-hand side of Eq. (12), $J(\vec{r})/2 \to J(\vec{r})/4$; (iii) in Eq. (13), $a \to 2a$. The previous simulations were carried for this rescaled parameter.

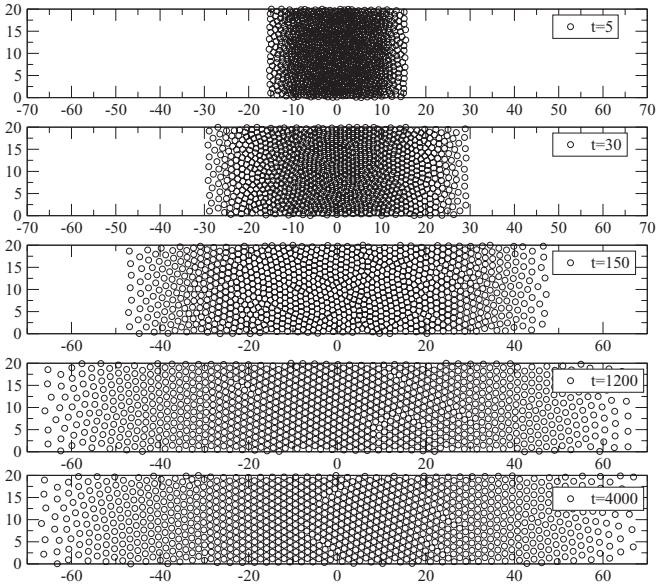

FIG. 1. Snapshots showing the particle positions at typical times t, for a single sample of $N = 1000$ particles. In each snapshot, the horizontal and vertical axes (x/λ and y/λ, respectively) show the relevant part of a box of size $L_x = 280\lambda$ and $L_y = 20\lambda$. At $t = 5$ the state is very close to the initial distribution, whereas the stationary state is almost reached at $t = 1200$. The time is dimensionless, measured in terms of the molecular-dynamics time step δt, as described in the text.

stationary state. As usual, the time is dimensionless, measured in terms of the integration time step δt, characteristic of the molecular-dynamics procedure. We have varied δt depending on the average velocities of the particles: for smaller times ($0 < t < 5$), i.e., in the high-velocity regime, we considered $\delta t = 10^{-3}$; for intermediate times ($5 \leqslant t < 150$), $\delta t = 10^{-2}$; in the slow-velocity regime ($t \geqslant 150$), we used $\delta t = 10^{-1}$. As an illustration of this time evolution, we exhibit in Fig. 1 snapshots of the particle positions for typical times t of a single sample with $N = 1000$ particles. At the smallest time shown ($t = 5$), one has a situation very close to the initial distribution, whereas for $t = 1200$ the system is very close to the stationary state. However, we have verified that the stationary state, where all particles typically stop moving, is attained only for $t \approx 3000$.

For any desired time t of the simulation, one can compute the corresponding profile for the density of particles $\rho(x,t)$, considering averages over samples. These results should be compared with the theoretical prediction given by the solution of Eq. (20); since $P(x,t) = (L_y/N)\rho(x,t)$, Eqs.(11)–(13) lead to

$$\rho(x,t) = \frac{NB(t)\beta(t)}{L_y}\left[\frac{1}{\beta(t)} - x^2\right]_+, \tag{21}$$

where

$$\frac{NB(t)\beta(t)}{L_y} = \frac{\alpha}{2a}[1 + (K_2 - 1)e^{-3\alpha t}]^{-1}. \tag{22}$$

In Fig. 2 the results from the simulations (symbols) are compared to the above theoretical prediction (solid lines). In Fig. 2(a) we show density profiles for typical situations in the high- and intermediate-velocity regimes, whereas in Fig. 2(b) profiles of the approach to the stationary state are shown. It is important to remember that we obtained $a = 2\pi f_0 \lambda^3$ through the coarse-graining approximation; the theoretical curves of Fig. 2 were obtained from Eqs. (21) and (22) by setting $a = (5.87 \pm 0.02) f_0 \lambda^3$, where the error bars come from the best least-squares fits of the theoretical curves, at different times. Such disagreement with the analytical estimate, leading to a relative discrepancy around 7% on the parameter a, is attributed to the approximations carried in Eqs. (17) and (18).

In Fig. 3(a) we represent all data of Fig. 2 in a plot of $\rho(x,t)/\rho(0,t)$ versus $\lambda x \rho(0,t)$. Notice that in this representation the densities profiles do not show time dependence on the width, and data for all times collapse into a single universal curve; the solid line is a parabola $\rho(x,t)/\rho(0,t) = [1 - b\{\lambda x \rho(0,t)\}^2]_+$, with $b \approx 4.3 \times 10^{-5}$. Another important

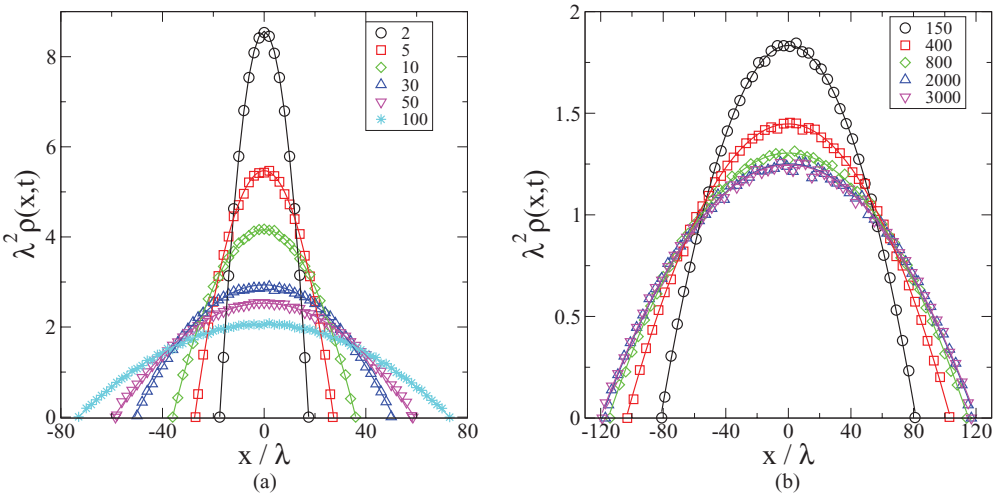

FIG. 2. (Color online) The dimensionless density of particles $\lambda^2\rho(x,t)$ is plotted versus x/λ, for typical times t: (a) short and intermediate times; (b) in the approach to the stationary state. The symbols are results from the simulations, whereas the solid lines represent the theoretical solution of the NLFPE, as given in Eqs. (21) and (22).

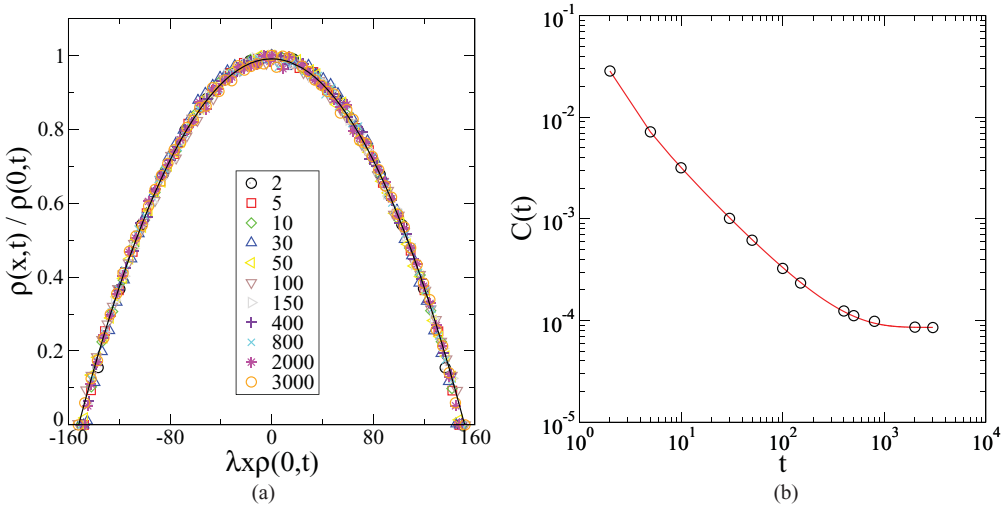

FIG. 3. (Color online) (a) Collapse of all data of Fig. 2 into a universal curve, using the representation $\rho(x,t)/\rho(0,t)$ versus $\lambda x\rho(0,t)$; the solid line is a parabola, as described in the text. (b) Time evolution of the dimensionless coefficient $C(t) = \lambda^4 N B(t)\beta(t)/L_y$; the empty circles are molecular-dynamics data, whereas the solid line corresponds to the theoretical prediction obtained from Eq. (22) by setting $a = 5.85 f_0 \lambda^3$. The time is dimensionless, measured in terms of the molecular-dynamics time step δt.

accordance found between the simulations and analytical results is shown in Fig. 3(b), where we present the time evolution of the dimensionless coefficient $C(t) = \lambda^4 N B(t)\beta(t)/L_y$, whose theoretical prediction is given in Eq. (22). The solid line corresponds to this analytical result by setting $a = 5.85 f_0 \lambda^3$, which is in full agreement with the value of a used for the curves in Fig. 2.

A strong support for q-Gaussian distributions is presented in Fig. 4, where we plot the q logarithm, $\ln_q u = (u^{1-q} - 1)/(1-q)$ $(u > 0)$ [6], for some typical times of Fig. 2 [Fig. 4(a)] as well as of the collapsed representation of Fig. 3(a) [Fig. 4(b)] in conveniently scaled variables. In this representation, q-Gaussian distributions become straight lines. In all cases the symbols, which represent the data from the simulations, show a good agreement with the straight line characteristic of the plot, considering the index $q = 0$.

In Ref. [10] the time dependence of the second moment $\langle x^2 \rangle$ of the q-Gaussian distribution in Eq. (2) was calculated [cf. Eq. (6)]. In Fig. 5 we present this quantity at different times of the evolution process, as computed from our simulations. For short times one finds the expected anomalous-diffusion regime, $\langle x^2 \rangle \sim t^{2/3}$, and deviations from this regime are found for longer times, where the confining potential drives the system toward its stationary state. The line corresponds to the analytical result of Eq. (6), showing a good agreement with the simulations for all times.

All numerical data presented so far are related to the distribution $P(x,t)$. They provide strong evidence that the time evolution of the system of vortices defined above should be described appropriately by means of the NLFPE in Eq. (20); its solution, given in Eq. (11), corresponds to a q-Gaussian distribution with $q = 0$. From now on, we will be concerned

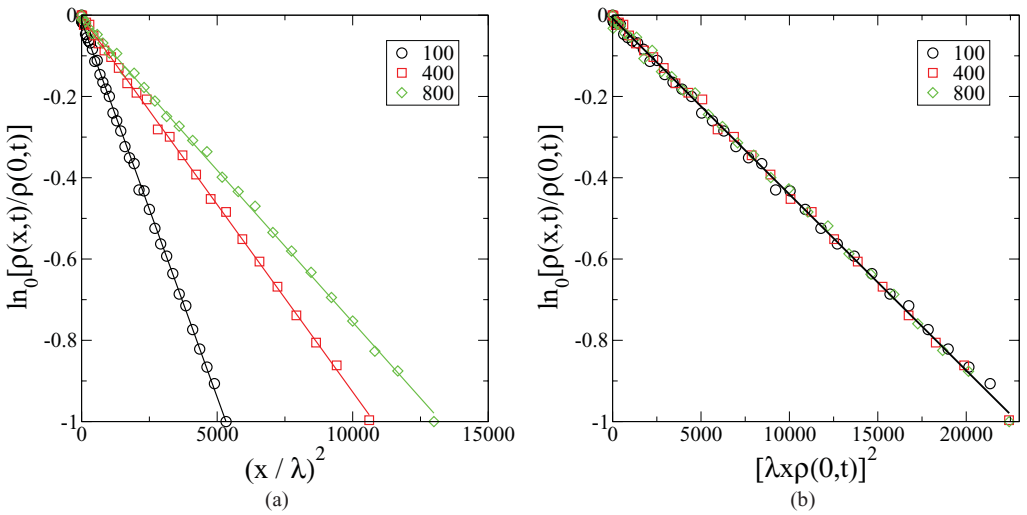

FIG. 4. (Color online) Plots of $\ln_0[\rho(x,t)/\rho(0,t)]$ versus dimensionless abscissas for some typical times: (a) three times from Fig. 2; (b) the same times from the collapsed representation of Fig. 3(a). The straight lines correspond to the analytical results obtained from Eq. (21).

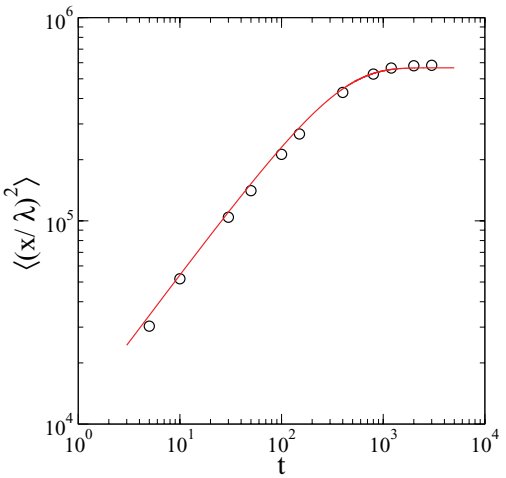

FIG. 5. (Color online) Time behavior of the dimensionless second moment $\langle (x/\lambda)^2 \rangle$; for short times we verified an anomalous diffusion characterized by $\langle x^2 \rangle \sim t^{2/3}$. The symbols are data from the simulations, whereas the line corresponds to the analytical calculation of Eq. (6) with $\nu = 2$.

with the time behavior of the corresponding velocities v_x. It should pointed out that, in this case, to our knowledge there is no analytical result for the associated probability distributions; therefore, the following results are only numerical.

Since for the conditions considered at the initial time all particles are located close to the origin, around which the harmonic potential is very weak, the prevalence of the repulsive interactions make the particles move away from the origin rapidly in the x direction, leading to possible large values for the corresponding velocities $\{v_{ix}\}$ $(i = 1,2,\ldots,N)$. After some time, the confining potential starts playing an important role, and its main effect is to decrease these velocities until they reach the stationary state shown in Fig. 1. We have investigated the time evolution of the probability distribution $P(v_x,t)$, associated with the velocities $\{v_{ix}\}$, and the results are exhibited in Fig. 6. It should be mentioned that herein the time is dimensionless, measured in terms of the molecular-dynamics time step δt, and so velocities are presented with a dimension of length. As expected, these distributions present

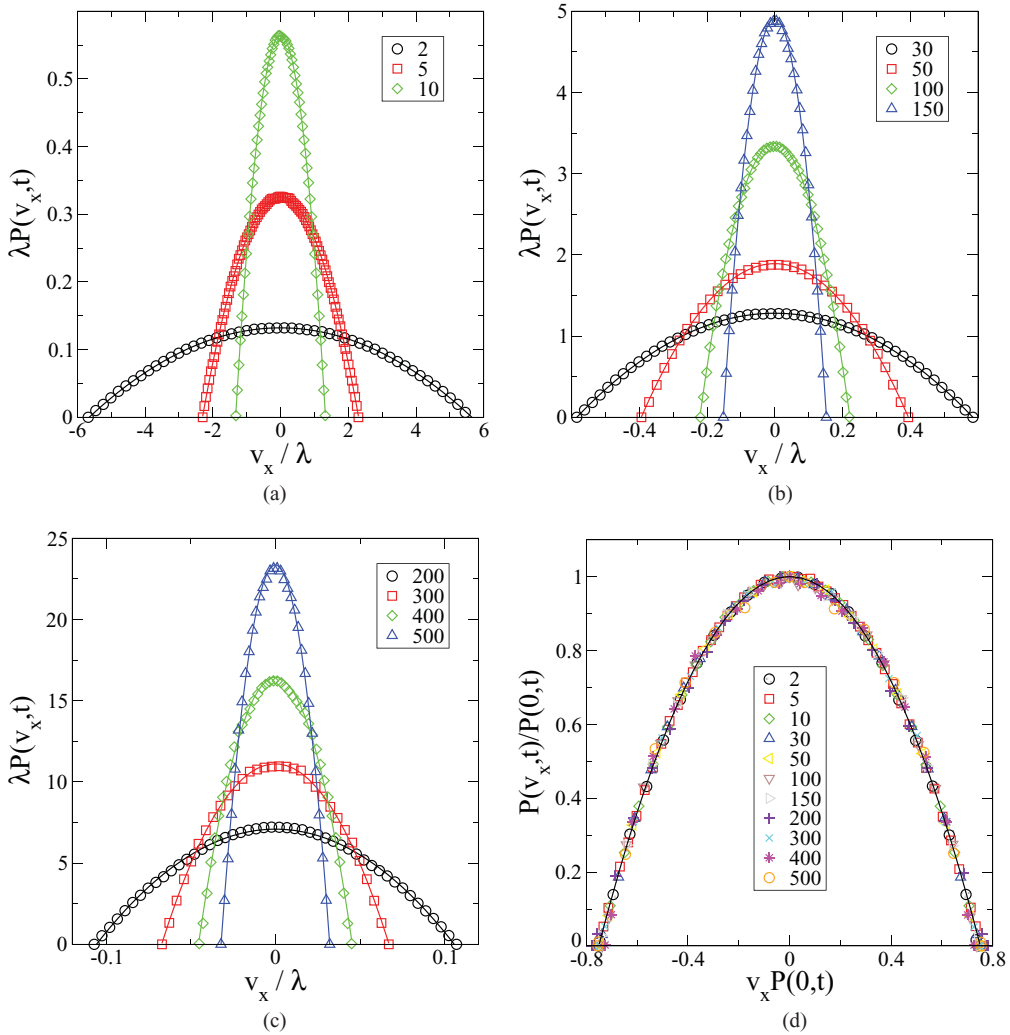

FIG. 6. (Color online) The dimensionless probability distributions $\lambda P(v_x,t)$ versus v_x/λ is exhibited for typical increasing times: (a) at the beginning of the evolution; (b) intermediate times; (c) in the approach to the stationary state. All these data fall into a universal curve, for conveniently rescaled variables, as shown in (d). Since time is dimensionless, velocities are presented with a dimension of length. The symbols represent simulation data, whereas solid curves are q-Gaussian distributions with $q = 0$.

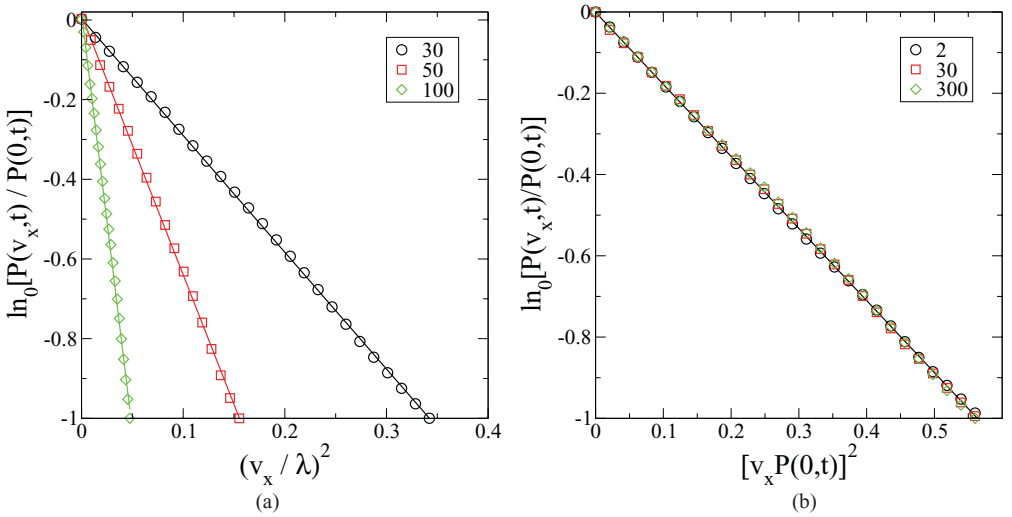

FIG. 7. (Color online) Plots of $\ln_0[P(v_x,t)/P(0,t)]$ versus dimensionless abscissas for some typical times: (a) three times from Fig. 6(b); (b) three typical times from the collapsed representation of Fig. 6(d). The straight lines are guides to the eye.

larger widths at the beginning of the evolution and they become narrow as time increases, approaching a delta function for sufficiently large times, i.e., $\lim_{t\to\infty} P(v_x,t) = \delta(v_x)$ [cf., e.g., the case $t = 500$ in Fig. 6(c)]. However the most interesting conclusion of Fig. 6 concerns the fact that the velocities $\{v_{ix}\}$ follow q-Gaussian distributions similar to the positions $\{x_i\}$,

$$P(v_x,t) = B_v(t)\left[1 - \beta_v(t)v_x^2\right]_+, \tag{23}$$

where we have introduced the time-dependent parameters $B_v(t)$ and $\beta_v(t)$ in correspondence with Eq. (11). This evidence is given by the good agreement between the numerical data and the solid lines in Fig. 6. In the collapsed representation, the solid line represents a universal parabola, $P(v_x,t)/P(0,t) = [1 - b\{v_x P(0,t)\}^2]_+$, with $b \approx 1.77$. Further indication for the behavior of Eq. (23) is given in Fig. 7, where we present plots of $\ln_0[P(v_x,t)/P(0,t)]$ versus dimensionless abscissas for some typical times chosen either from Fig. 6(b) [leading to the plots of Fig. 7(a)] or from the collapsed data of Fig. 6(d) [yielding the plot of Fig. 7(b)]. The results shown above strongly suggest that the same index $q = 0$ applies for both distributions $P(x,t)$ and $P(v_x,t)$; the distribution $P(x,t)$ found herein is supported by a previously studied NLFPE, whereas $P(v_x,t)$ still lacks an appropriate theoretical background.

Similarly to what was done in the case of positions, where we examined the product of the time-dependent coefficients $B(t)$ and $\beta(t)$ [cf. Fig 3(b)], we have also investigated the time evolution of the dimensionless quantity $\lambda^3 B_v(t)\beta_v(t)$, as presented in Fig. 8. Analogous to those quantities shown in Figs. 3(b) and 5, one sees two distinct time behaviors: a short-time regime where $\lambda^3 B_v(t)\beta_v(t) \sim t^{5/2}$, followed by a different behavior in the approach toward the stationary state.

IV. CONCLUSION

We have studied a system of interacting vortices under an overdamped motion, which has been commonly used in the literature to model flux-front penetration in disordered type-II superconductors. In a previous work [18], this model was related to a nonlinear Fokker-Planck equation, typical of nonextensive statistical mechanics in a two-fold way: (i) analytically, through a coarse-graining approximation; and (ii) numerically, by showing that the stationary-state solution of this equation was in good agreement with results obtained from molecular-dynamics simulations. Herein, this relation has been extended by showing that it holds along the whole time evolution, with the probability distribution for the positions, $P(x,t)$, given by a q Gaussian with $q = 0$ (i.e., a parabola), for all times. Along its time evolution $P(x,t)$ spreads in time (keeping fixed the value of q), and its width, normalization, and second moment were shown to be in full agreement with the analytic solution of the nonlinear Fokker-Planck equation. The present results strongly reinforce the approach used in Ref. [18] and corroborate the reply in Ref. [19].

Moreover, we have also presented results for the x-component velocity probability distribution $P(v_x,t)$,

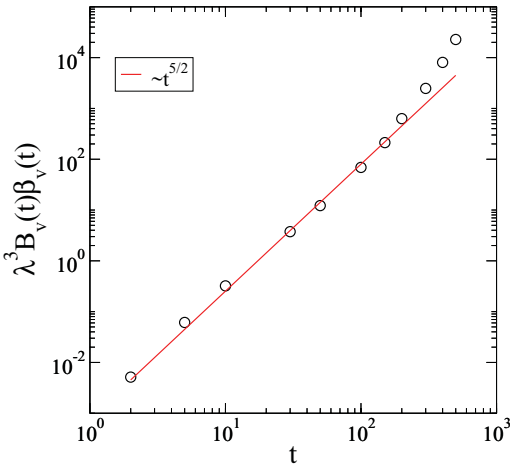

FIG. 8. (Color online) Time evolution of the dimensionless coefficient $\lambda^3 B_v(t)\beta_v(t)$, defined in Eq. (23). The symbols are data from the simulations, whereas the solid straight line presents a slope of 5/2.

showing that it is given by a q-Gaussian distribution totally analogous to $P(x,t)$, with the same value of q, namely $q = 0$. However, contrary to $P(x,t)$, the distribution $P(v_x,t)$ shrinks in time, approaching a delta function as the system evolves toward the stationary state. In contrast to $P(x,t)$, for which there is a theoretical background in accordance with the present results, we are not aware of any theoretical analysis related to the distribution $P(v_x,t)$. This may be given by a kind of nonlinear Kramers equation involving a joint probability distribution $P(x,v_x,t)$, from which the distributions found herein would represent marginal probabilities; analytical investigations in this direction are welcome.

To summarize, we have presented broad evidence that a system of interacting vortices under overdamped motion constitutes an important physical application for nonextensive statistical mechanics. Its time-dependent properties, in addition to those of the stationary state, were shown to be fully compatible with this theory.

ACKNOWLEDGMENTS

We thank CAPES, CNPq, and FAPERJ (Brazilian Agencies) for financial support. We are grateful to Constantino Tsallis, J. S. Andrade Jr., and A. A. Moreira for fruitful conversations.

[1] *Encyclopedia of Nonlinear Science*, edited by A. C. Scott (Taylor and Francis, New York, 2005).
[2] A. C. Scott, *The Nonlinear Universe* (Springer, Berlin, 2007).
[3] C. Sulem and P.-L. Sulem, *The Nonlinear Schrödinger Equation: Self-Focusing and Wave Collapse* (Springer, New York, 1999).
[4] T. D. Frank, *Nonlinear Fokker-Planck Equations: Fundamentals and Applications* (Springer, Berlin, 2005).
[5] F. D. Nobre, M. A. Rego-Monteiro, and C. Tsallis, Phys. Rev. Lett. **106**, 140601 (2011).
[6] C. Tsallis, *Introduction to Nonextensive Statistical Mechanics* (Springer, New York, 2009).
[7] A. R. Plastino and A. Plastino, Physica A **222**, 347 (1995).
[8] C. Tsallis and D. J. Bukman, Phys. Rev. E **54**, R2197 (1996).
[9] L. E. Reichl, *A Modern Course in Statistical Physics*, 2nd ed. (John Wiley and Sons, New York, 1998).
[10] V. Schwämmle, E. M. F. Curado, and F. D. Nobre, Eur. Phys. J. B **70**, 107 (2009).
[11] T. D. Frank and A. Daffertshofer, Physica A **272**, 497 (1999).
[12] T. D. Frank and A. Daffertshofer, Physica A **295**, 455 (2001).
[13] P. H. Chavanis, Phys. Rev. E **68**, 036108 (2003).
[14] P. H. Chavanis, Physica A **340**, 57 (2004).
[15] V. Schwämmle, F. D. Nobre, and E. M. F. Curado, Phys. Rev. E **76**, 041123 (2007).
[16] V. Schwämmle, E. M. F. Curado, and F. D. Nobre, Eur. Phys. J. B **58**, 159 (2007).
[17] M. S. Ribeiro, F. D. Nobre, and E. M. F. Curado, Entropy **13**, 1928 (2011).
[18] J. S. Andrade Jr., G. F. T. da Silva, A. A. Moreira, F. D. Nobre, and E. M. F. Curado, Phys. Rev. Lett. **105**, 260601 (2010).
[19] Y. Levin and R. Pakter, Phys. Rev. Lett. **107**, 088901 (2011); J. S. Andrade Jr., G. F. T. da Silva, A. A. Moreira, F. D. Nobre, and E. M. F. Curado, *ibid*. **107**, 088902 (2011).
[20] H. J. Jensen, A. Brass, and A. J. Berlinsky, Phys. Rev. Lett. **60**, 1676 (1988).
[21] O. Pla and F. Nori, Phys. Rev. Lett. **67**, 919 (1991).
[22] R. A. Richardson, O. Pla, and F. Nori, Phys. Rev. Lett. **72**, 1268 (1994).
[23] S. Zapperi, A. A. Moreira, and J. S. Andrade, Phys. Rev. Lett. **86**, 3622 (2001).